

# Experimental band structure of the nearly half-metallic $\text{CuCr}_2\text{Se}_4$ : An optical and magneto-optical study

S. Bordács,<sup>1,2</sup> I. Kézsmárki,<sup>1,2,3</sup> K. Ohgushi,<sup>4</sup> and Y. Tokura<sup>2,3</sup>

<sup>1</sup>*Department of Physics, Budapest University of Technology and Economics and Condensed Matter Research Group of the Hungarian Academy of Sciences, 1111 Budapest, Hungary*

<sup>2</sup>*Multiferroics Project, ERATO, Japan Science and Technology Agency (JST), Japan c/o Department of Applied Physics, The University of Tokyo, Tokyo 113-8656, Japan*

<sup>3</sup>*Department of Applied Physics, University of Tokyo, Tokyo 113-8656, Japan*

<sup>4</sup>*Institute for Solid State Physics, University of Tokyo, Kashiwanoha, Kashiwa, Chiba 277-8581, Japan*

(Dated: February 28, 2022)

Diagonal and off-diagonal optical conductivity spectra have been determined from the measured reflectivity and magneto-optical Kerr effect (MOKE) over a broad range of photon energy in the itinerant ferromagnetic phase of  $\text{CuCr}_2\text{Se}_4$  at various temperatures down to  $T=10$  K. Besides the low-energy metallic contribution and the lower-lying charge transfer transition at  $E \approx 2$  eV, a sharp and distinct optical transition was observed in the mid-infrared region around  $E=0.5$  eV with huge magneto-optical activity. This excitation is attributed to a parity allowed transition through the Se-Cr hybridization-induced gap in the majority spin channel. The large off-diagonal conductivity is explained by the high spin polarization in the vicinity of the Fermi level and the strong spin-orbit interaction for the related charge carriers. The results are discussed in connection with band structure calculations.

PACS numbers:

## I. INTRODUCTION

The ferrimagnetic metal  $\text{CuCr}_2\text{Se}_4$  shows the highest critical temperature  $T_c=430$  K among chromium spinel chalcogenides.<sup>1</sup> Although the lattice constants of the ferromagnetic semiconductors  $\text{CdCr}_2\text{S}_4$  and  $\text{CdCr}_2\text{Se}_4$  differ only by 1-4%, their ferromagnetism is considerably weakened by the complete filling of the valance band as reflected by  $T_c=85$  K and 129 K, respectively<sup>1</sup>.  $\text{CuCr}_2\text{Se}_4$  exhibits large magneto-optical Kerr effect (MOKE) in the near infrared photon energy region at room temperature which makes this compound a promising candidate for magneto-optical devices.<sup>2</sup> Materials from the same family show interesting magneto-transport phenomena like the colossal magnetoresistance<sup>3</sup> in  $\text{Fe}_{1-x}\text{Cu}_x\text{Cr}_2\text{S}_4$ , and the colossal magnetocapacitance<sup>4</sup> in  $\text{CdCr}_2\text{S}_4$ . Moreover, recent band structure calculations indicate that  $\text{CuCr}_2\text{Se}_4$  is almost half-metallic,<sup>5,6,7</sup> and the density of states for spin down electrons can be fully suppressed with cadmium doping, i.e. a perfect half-metallic situation can be realized.<sup>7</sup>

The strong ferrimagnetism in  $\text{CuCr}_2\text{Se}_4$  was first explained by Lotgering and Stapele assuming the mixed-valence state of  $\text{Cr}^{3+}$  and  $\text{Cr}^{4+}$  with the monovalent  $\text{Cu}^+$ ; thus, this compound was classified as a d-metal with closed Se 4p shell.<sup>8</sup> In this picture only the chromium sites are magnetic and the double exchange mechanism between the  $\text{Cr}^{3+}$  and the  $\text{Cr}^{4+}$  ions align their magnetic moment parallel. However, early neutron diffraction studies indicated that each chromium is in the  $\text{Cr}^{3+}$  state.<sup>9</sup> Later, Goodenough proposed the copper ions to be divalent  $\text{Cu}^{2+}$  and as a source of the magnetism the 90 degree superexchange to be responsible for the coupling between the  $\text{Cr}^{3+}$  ions through the completely filled Se 4p

states.<sup>10</sup> The recent XMCD measurements by Kimura et al.<sup>11</sup> settled the long standing issue of the valance state of  $\text{CuCr}_2\text{Se}_4$ . They have confirmed the  $\text{Cr}^{3+}$  state, however, they have found almost monovalent copper and a delocalized hole in the Se 4p band with a magnetic moment anti-parallel to the moment of the  $\text{Cr}^{3+}$  ions. Based on these experimental results Sarma et al.<sup>6</sup> have interpreted the ferrimagnetism in terms of a kinetic-energy driven mechanism in which the hybridization between the localized  $\text{Cr}^{3+}$  ions and the delocalized Se 4p band results a hole mediated exchange. Their density functional calculation indicates the appearance of a hybridization induced hump-like structure at the Fermi energy only for the up spin states in accordance with other band structure calculations.<sup>5,7</sup>

In order to have a deeper understanding of the electronic structure of  $\text{CuCr}_2\text{Se}_4$  we have investigated the low-energy ( $E=0.1-4$  eV) charge excitations over the temperature range of  $T=10-300$  K by determining both diagonal and off-diagonal element of the optical conductivity tensor. Beside the low-energy response of the metallic carriers and the charge transfer excitations above  $E \gtrsim 2$  eV, we have found a sharp and distinct optical transition in the mid-infrared region with large magneto-optical activity.

## II. EXPERIMENTAL

Single crystals of  $\text{CuCr}_2\text{Se}_4$  were grown by the chemical vapor transport method. Details of the preparation and the structure characterization were given elsewhere.<sup>12</sup> All the optical measurements were carried out with nearly normal incidence on the as-grown (111)



surface. In order to determine the diagonal optical conductivity, reflectivity spectra was measured over a broad energy range ( $E=0.08\text{--}26\text{ eV}$  and  $E=0.08\text{--}5\text{ eV}$  at room and low temperature, respectively) to facilitate the proper Kramers-Kronig transformation. We have measured the complex magneto-optical Kerr angle  $\Phi_{Kerr} = \theta_{Kerr} + i\eta_{Kerr}$ , which allows the direct determination of the off-diagonal conductivity, between  $E=0.12\text{--}4\text{ eV}$  with a polarization modulation technique.<sup>13</sup> In the mid-infrared region a Fourier transform infrared spectrometer was combined with a ZnSe photoelastic modulator (Hinds, II/ZS50)<sup>12</sup> to perform measurements down to as low energy as  $E=0.12\text{ eV}$ , while above  $E > 0.7\text{ eV}$  a  $\text{CaF}_2$  photoelastic modulator (Hinds, I/CF50) and a grating spectrometer was used. The external magnetic field  $B=\pm 0.25\text{ T}$  was applied by a permanent magnet along the  $[111]$  easy axis of the magnetization and also parallel to the propagation direction of the light. In the above arrangement, the conductivity tensor has the following form:

$$\underline{\underline{\sigma}} = \begin{bmatrix} \sigma_{xx} & \sigma_{xy} & 0 \\ -\sigma_{xy} & \sigma_{xx} & 0 \\ 0 & 0 & \sigma_{zz} \end{bmatrix}, \quad (1)$$

in our notation the x, y, z directions do not correspond to the main cubic axes, as z is chosen parallel to the  $[111]$  easy axis.

### III. RESULTS AND DISCUSSION

The temperature dependence of the reflectivity and the diagonal optical conductivity spectra is shown in Fig. 1. We identified the different contributions to the optical conductivity as follows. The first charge transfer peak is centered around  $E=2.75\text{ eV}$ , that we assign to  $\text{Se } 4p \rightarrow \text{Cr } 3d$  transition in agreement with former optical data on a broad variety of chromium spinel oxides and chalcogenides.<sup>12</sup> It has a low-energy shoulder located at  $E=1.9\text{ eV}$  which likely originates from the on-site chromium d-d transition since this structure is common for chromium spinels insensitive to the change of the other cation.<sup>12</sup> This originally dipole-forbidden transition becomes allowed by the hybridization with the ligand, which results in the fairly small oscillatory strength. The spectral structures become distinct as the temperature decreases. In the low-energy region ( $E \lesssim 0.1\text{ eV}$ ) metallic conductivity appears. Although it does not closely follow a Drude-like behaviour – the scattering rate is estimated to be  $\gamma \approx 0.03\text{ eV}$  at  $T=10\text{ K}$  – the small residual resistivity<sup>12</sup>  $\rho_o = 10\ \mu\Omega\text{cm}$  is not typical of bad metals with strongly correlated d band. Between the low-energy metallic term and the first charge transfer excitation, a distinct peak appears at  $E=0.5\text{ eV}$ . At low temperatures it becomes clearly distinguishable from the excitation of the free carriers. In spite of its closeness to the metallic continuum it becomes sharp at low temperatures characterized by a width of  $\Gamma \approx 0.5\text{ eV}$  width. In the inset of

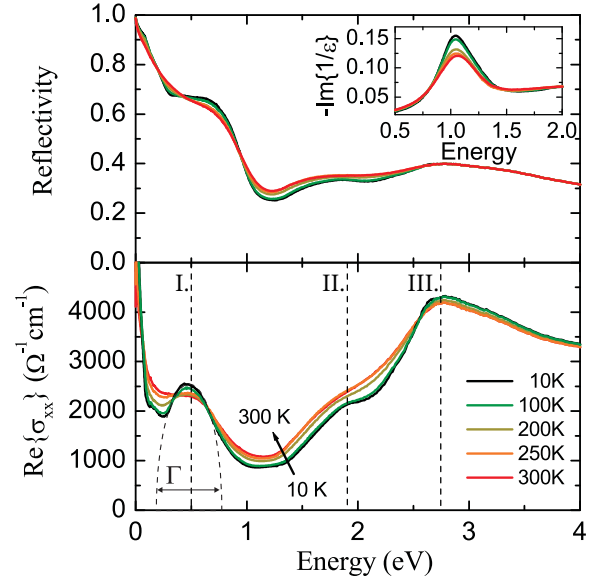


FIG. 1: (Color online) Upper and lower panel: The reflectivity and the optical conductivity spectra of  $\text{CuCr}_2\text{Se}_4$  at various temperatures. Three main features are indicated by dashed lines. The first charge transfer excitation ( $\text{Se } 4p \rightarrow \text{Cr } 3d$ ) appears at  $E=2.75\text{ eV}$  with a low-energy shoulder at  $E=1.9\text{ eV}$  due to on-site d-d transition of the chromium ions. In addition to the low-energy metallic peak, a strong transition is present in the mid-infrared region (at  $E=0.5\text{ eV}$ ) with a characteristic width of  $\Gamma \approx 0.5\text{ eV}$ . In the inset the maximum of the loss-function indicates the plasma frequency at  $\hbar\omega_{pl} \approx 1\text{ eV}$ .

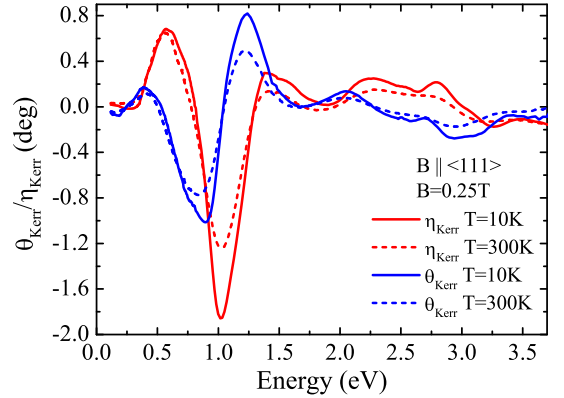


FIG. 2: (Color online) The spectra of the magneto-optical Kerr parameters at room temperature and  $T=10\text{ K}$ . The Kerr ellipticity shows a peak at  $E=1\text{ eV}$  due to the plasma resonance and its maximal value increase to  $\eta_{Kerr}=1.9^\circ$  as the temperature decrease to  $T=10\text{ K}$  corresponding to the sharpening of the plasma edge. The Kerr rotation reaches the value  $\theta_{Kerr}=1.2^\circ$  in the same region.

Fig. 1 the maximum of the loss-function signals a plasma frequency of  $\hbar\omega_{pl} \approx 1\text{ eV}$ , which only increase by 4% as the temperature decrease to  $T=10\text{ K}$ . This implies merely tiny changes in the carrier concentration as a function of temperature.

The magneto-optical Kerr spectra are presented in



Fig. 2 at room temperature and at the lowest temperature  $T=10$  K. These results are in good agreements with Kerr spectra previously reported at room-temperature for  $E>0.6$  eV.<sup>2</sup> The MOKE signal reaches its maximum around  $E=1$  eV, where Kerr ellipticity exhibits a peak while Kerr rotation has a dispersive line shape with the maximal values of  $\eta_{Kerr}=1.9^\circ$  and  $\theta_{Kerr}=-1^\circ$ , respectively. Although the magnetization is almost constant below room temperature, the MOKE is enhanced by 45% down to  $T=10$  K.

From the complex Kerr angle, we have calculated the off-diagonal conductivity according to the following relation:

$$\Phi_{Kerr} = \theta_{Kerr} + i\eta_{Kerr} = -\frac{\sigma_{xy}}{\sigma_{xx}\sqrt{1 + \frac{4\pi i}{\omega}\sigma_{xx}}}, \quad (2)$$

where  $\sigma_{xx}$  and  $\sigma_{xy}$  are the elements of the complex optical conductivity tensor. The Kerr rotation and ellipticity describe the phase-shift and the intensity difference, respectively, between left and right circularly polarized light upon normal-incidence reflection from a magnetic surface. The corresponding results are presented in Fig. 3.

In spite of the large MOKE around  $E=1$  eV, neither the off-diagonal nor the diagonal conductivity show any specific optical excitation in this energy region. The large enhancement of the MOKE signal corresponds to the plasma resonance at  $\hbar\omega_{pl} \approx 1$  eV; it is caused by the strong minimum of the denominator of Eq. 2 rather than by an increase of the off-diagonal conductivity.<sup>2,14</sup> The almost perfect cancelation of this resonance in the off-diagonal conductivity indicates the properness of the Kramers-Kronig transformation for the reflectivity. When the optical excitations are broad compared to the magnetically induced splitting of these transitions for the two circular polarizations, the Kerr parameters  $\theta_{Kerr}$  and  $\eta_{Kerr}$  are proportional to the derivative of the reflectivity:

$$\eta_{Kerr} = \frac{1}{2} \frac{r_+^2 - r_-^2}{r_+^2 + r_-^2} \propto \frac{1}{R(E)} \frac{\partial R(E)}{\partial E}$$

$$\theta_{Kerr} = \frac{1}{2} (\phi_+ - \phi_-) \propto \frac{\partial \phi(E)}{\partial E}, \quad (3)$$

where  $\tilde{r}_\pm = r_\pm e^{i\phi_\pm}$  are the Fresnel coefficients for the right and left circularly polarized photons and  $R(E) = (r_+^2 + r_-^2)/2$  and  $\phi(E)$  are the reflectivity and the corresponding phase. The sudden decrease of the reflectivity near the plasma edge, which generate the large MOKE signal, is sensitive to the slope of the reflectivity which becomes steeper as the life-time increases toward low temperatures, causing considerable temperature dependence in the region of the plasma resonance.

The real part of the off-diagonal conductivity (shown in Fig. 3) is dominated by two main structures, namely a broader hump around  $E=2.75$  eV and a resonance-like peak centered at  $E=0.5$  eV. The dispersive line-shape in the imaginary part of the off-diagonal conductivity and also the corresponding large values –

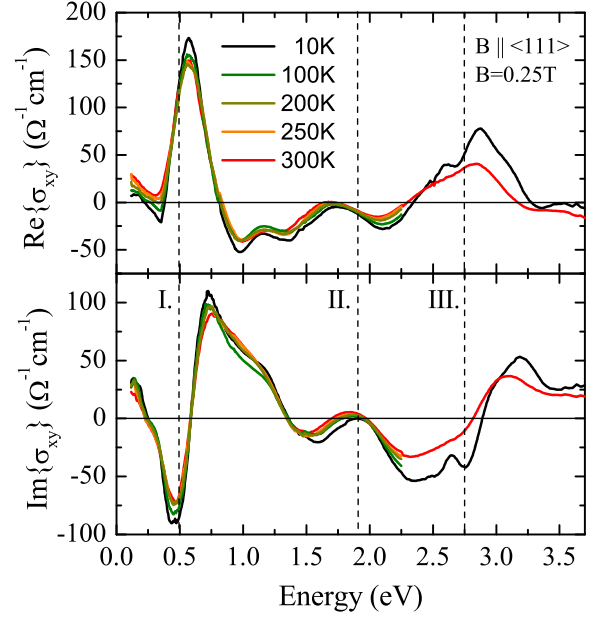


FIG. 3: (Color online) The off-diagonal conductivity determined from the magneto-optical Kerr spectra. The plasma edge resonance observed in the Kerr effect is cancelled out, which indicate that the Kramers-Kronig transformation was performed properly. The dashed lines with labels indicates the same transition like in Fig. 1. The transition at  $E=0.5$  eV shows large while the Se 4p→Cr 3d charge transfer excitation has also considerable magneto-optical activity.

$\text{Im}\{\sigma_{xy}\}=53 \Omega^{-1} \text{cm}^{-1}$  and  $\text{Im}\{\sigma_{xy}\}=110 \Omega^{-1} \text{cm}^{-1}$  at  $T=10$  K, respectively – are suggestive of parity allowed transitions, which is reasonable for the Se 4p→Cr 3d charge transfer transition at  $E=2.75$  eV. The magnitude of the low-energy part of the off-diagonal conductivity enlarged in Fig. 4. is very close to that of the dc Hall effect obtained in the same magnetic field,<sup>15</sup> except for  $T=10$  K where  $\sigma_{Hall}=300 \Omega^{-1} \text{cm}^{-1}$ . As the temperature decreases the low-energy tail of the real part is considerably reduced in contrast to the temperature independent behavior of the magnetization. This may indicate that a non-perturbative treatment of the spin-orbit coupling is also necessary to describe the low-energy off-diagonal conductivity as it was formerly proposed for the dc anomalous Hall effect.<sup>15,16</sup>

The relations between the elements of the optical conductivity tensor and the underlying microscopic optical processes are described by the Kubo formula:

$$\text{Re}\{\sigma_{xx}\} = \frac{\pi e^2}{2m^2 V \hbar \omega} \sum_{i,f} [1 - f(\epsilon_f)] f(\epsilon_i) \{ |\langle f | \Pi_+ | i \rangle|^2 + |\langle f | \Pi_- | i \rangle|^2 [\delta(\omega_{fi} - \omega) + \delta(\omega_{fi} + \omega)] \},$$

$$\text{Im}\{\sigma_{xy}\} = \frac{\pi e^2}{4m^2 V \hbar \omega} \sum_{i,f} [1 - f(\epsilon_f)] f(\epsilon_i) \{ |\langle f | \Pi_+ | i \rangle|^2 - |\langle f | \Pi_- | i \rangle|^2 [\delta(\omega_{fi} - \omega) + \delta(\omega_{fi} + \omega)] \}, \quad (4)$$

where  $\Pi_\pm = \Pi_x \pm i\Pi_y$  are the momentum operators in cir-



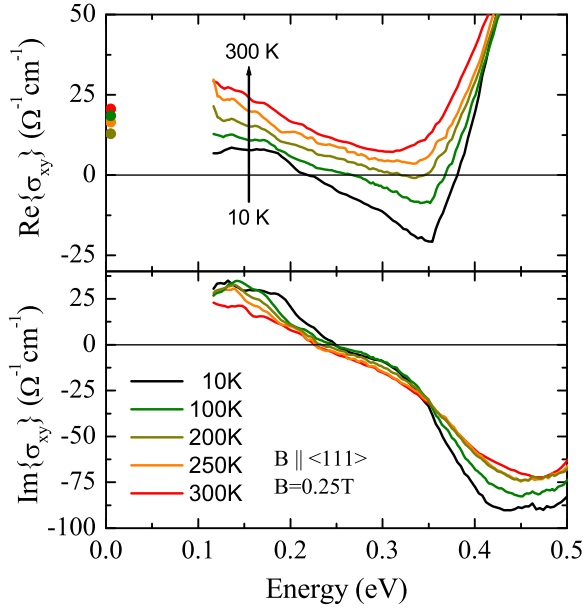


FIG. 4: (Color online) The low-energy part of the off-diagonal conductivity. The dc values are reproduced from Hall resistivity measurement performed in the same magnetic field by Lee et al.<sup>15</sup>

cular basis. The real part of the diagonal optical conductivity is proportional to the joint density of states for the occupied and unoccupied states multiplied by the electric dipole matrix elements, therefore, it describes the absorption of light for left and right circularly polarized photons in average. On the other hand, the off-diagonal conductivity is the difference between the absorption spectra corresponding the two circular polarizations. Contributions from electric dipole processes to off-diagonal optical conductivity are remarkable in ferromagnetic materials – due to the orbital magnetization induced by the spontaneous spin polarization via the spin-orbit interaction – similarly to the anomalous Hall effect in the dc limit.

To understand the origin of the optical excitations, the results of the recent band structure calculations<sup>5,6,7</sup> are summarized schematically in Fig. 5. The chromium d-band is split by the cubic crystal field to a  $t_{2g}$  and an  $e_g$  band. The selenium 4p and the copper 3d states are fully mixed with each other. Furthermore, the hybridization between the selenium 4p and the chromium  $t_{2g}$  induces a gap just below the Fermi energy in the majority spin channel. As a consequence, states from the Se 4p band are shifted above the Fermi level (referred to as “hump in the density of states” in the introduction), thus holes appears in the majority spin channel. The main optical transitions observed in the experiments are also indicated in the figure.

Our optical and magneto-optical study confirms the results of the band structure calculations both in the close vicinity of the Fermi energy and on a few eV large scale. In agreement with the theoretical results, we explain the transition at  $E=0.5$  eV as excitations trough the

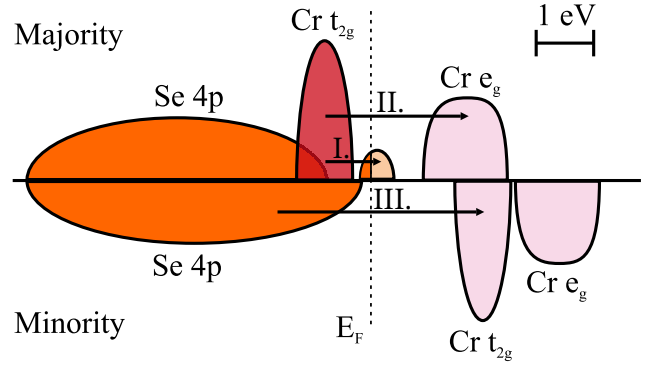


FIG. 5: (Color online) The schematic structure of the density of states as it determined by density functional calculations.<sup>5,6,7</sup> The chromium d-band is split by the cubic crystal field to a  $t_{2g}$  and an  $e_g$  band. The hybridization between the selenium and chromium induce a gap just below the Fermi energy and a holes appears in the majority spin channel. The arrows indicate the excitations observed both in the diagonal and off-diagonal conductivity spectra with the same labels as used in Fig. 1 and 3.

hybridization induced gap. The high oscillator strength is due to the parity difference between the initial and the final states. The large off-diagonal conductivity is possibly owing to the strong spin-orbit coupling for the delocalized electrons with strong selenium character ( $E_{SO} \approx 0.5$  eV) and the highly spin polarized states in the  $\sim 1$  eV vicinity of the Fermi level.<sup>5,7</sup> The first charge transfer excitations around  $E=2.75$  eV, with a remarkable oscillator strength and magneto-optical activity are attributed to Se 4p  $\rightarrow$  Cr 3d transition, while the excitation at  $E=1.9$  eV is assigned to on-site d-d transitions of chromium ions. These are in overall agreement with the numerical calculations, although the transition energies are somewhat higher in the experiment.<sup>5,6,7</sup> The contribution of the d-d transition to the off-diagonal conductivity is small compared to that of the charge transfer transition. Besides the reduced oscillator strength of the d-d transition due to its dipole forbidden nature, it is likely caused by the fairly small spin-orbit coupling for chromium ( $E_{SO}=0.09$  eV).<sup>5</sup>

The measurement of the off-diagonal conductivity greatly helps to extract the optical transition found around  $E=0.5$  eV since its large magneto-optical activity dominates over the contribution from the metallic charge carriers (damped cyclotron resonance) contrary to the case of the diagonal conductivity.

#### IV. CONCLUSIONS

We have measured the reflectivity and magneto-optical Kerr effect over a broad energy range ( $E=0.08-26$  eV and  $E=0.1-4$  eV, respectively) at various temperatures down to  $T=10$  K and evaluated the elements of the optical conductivity tensor. The diagonal and off-diagonal optical conductivity spectra determined from the experiments



are consistent with the results of former band structure calculations<sup>5,6,7</sup> over the whole energy region. At low energies a metallic peak is present, while the  $E \gtrsim 2$  eV region is dominated by the first charge transfer transition Se 4p $\rightarrow$ Cr 3d. Moreover, we have observed a distinct optical transition around  $E=0.5$  eV that we attribute to excitations through the Se-Cr hybridization induced gap. This transition has huge magneto-optical activity due to the high spin polarization in the  $\sim 1$  eV vicinity of the

Fermi level and its parity-allowed nature. The corresponding sharp feature in the off-diagonal conductivity dominates over the contribution from the metallic electrons. Large enhancement of the Kerr effect was also observed around the plasma edge.

This work was supported by a Grant-In-Aid for Scientific Research, MEXT of Japan, and the Hungarian Research Funds OTKA PD75615, NK72916, Bolyai 00256/08/11.

- 
- <sup>1</sup> Landolt-Börnstein, *Magnetic and other properties of oxides and related compounds*, Vol III. part 12b, Springer, Berlin (1988) and the references there.
- <sup>2</sup> H. Brändle, J. Schoenes, P. Wachter, F. Hulliger and W. Reim, *J. Magn. Magn. Mat.* **93**, 207 (1991).
- <sup>3</sup> A. P. Ramirez, R. J. Cava and J. Krajewski, *Nature* **386**, 156 (1997).
- <sup>4</sup> J. Hemberger, P. Lunkenheimer, R. Fichtl, H.-A. Krug von Nidda, V. Tsurkan and A. Loidl, *Nature* **434**, 364 (2005).
- <sup>5</sup> V. N. Antonov, V. P. Antropov, B. N. Harmon, A. N. Yaresko and A. Ya. Perlov, *Phys. Rev. B* **59**, 14552 (1999).
- <sup>6</sup> T. Saha-Dasgupta, Molly De Raychaudhury and D. D. Sarma, *Phys. Rev. B* **76**, 054441 (2007).
- <sup>7</sup> Y.-H. A. Wang, A. Gupta, M. Chshiev and W. H. Butler, *Appl. Phys. Lett.* **92**, 062507 (2008).
- <sup>8</sup> F. K. Lotgering and R.P. Stapele, *Solid State Commun.* **5**, 143 (1967).
- <sup>9</sup> C. Colominas, *Phys. Rev.* **153**, 558 (1966).
- <sup>10</sup> J. B. Goodenough, *J. Phys. Chem. Solids* **30**, 261 (1969).
- <sup>11</sup> A. Kimura, J. Matsuno, J. Okabayashi, A. Fujimori, T. Shishidou, E. Kulatov and T. Kanomata, *Phys. Rev. B* **63**, 224420 (2001).
- <sup>12</sup> K. Ohgushi, Y. Okimoto, T. Ogasawara, S. Miyasaka and Y. Tokura, *J. Phys. Soc. Jpn.* **77**, 034713 (2008).
- <sup>13</sup> K. Sato, *Jpn. J. Appl. Phys.* **20**, 2403 (1981).
- <sup>14</sup> H. Feil and C. Haas, *Phys. Rev. Lett.* **58**, 65 (1987).
- <sup>15</sup> Wei-Li Lee, S. Watauchi, V. L. Miller, R. J. Cava and N. P. Ong, *Science* **303**, 1647 (2004).
- <sup>16</sup> Y. Yao, Y. Liang, D. Xiao, Q. Niu, Shun-Qing Shen, X. Dai, and Z. Fang, *Phys. Rev. B* **75**, 020401(R) (2007).